

# A Deep Learning Mask Analysis Toolset Using SEM Digital Twins

Ajay Baranwal<sup>\*a</sup>, Suhas Pillai<sup>a</sup>, Thang Nguyen<sup>a</sup>, Jun Yashima<sup>b</sup>, Noriaki Nakayamada<sup>b</sup>, Mikael Wahlsten<sup>c</sup>, Aki Fujimura<sup>d</sup>

<sup>a</sup>Center for Deep Learning in Electronics Manufacturing, Inc. (cdle.ai);

<sup>b</sup>NuFlare Technology, Inc.; <sup>c</sup>Mycronic AB; <sup>d</sup>D2S, Inc.

## ABSTRACT

Sub-nanometer accuracy attainable with electron micrograph SEM images is the only way to “see” well enough for the mask analysis needed in EUV mask production. Because SEM images are pixel dose maps, deep learning (DL) offers an attractive alternative to the tedious and error-prone mask analysis performed by the operators and expert field application engineers in today’s mask shops. However, production demands preclude collecting a large enough variety and number of real SEM images to effectively train deep learning models. We have found that digital twins that can mimic the SEM images derived from CAD data provide an exceptional way to synthesize ample data to train effective DL models. Previous studies [1, 2, 3, 4] have shown how deep learning can be used to create digital twins. However, it was unclear if SEM images generated with digital twins would have sufficient quality to train a deep learning network to classify real SEM images. This paper shows how we built three DL tools for SEM-based mask analysis. The first tool automatically filters good quality SEM images, particularly for test chips, using a DL-based binary classifier. A second tool uses another DL model to align CAD and SEM images for applications where it is important that features on both the images are properly aligned. A third tool uses a DL multi-class classifier to categorize various types of VSB mask writer defects. In developing the three tools, we trained state-of-the-art deep neural networks on SEM images generated using digital twins to achieve accurate results on real SEM images. Furthermore, we validated the results of trained deep learning models through model visualization and accuracy-metric evaluation.

**Keywords:** photomask, mask analyses, SEM inspection, image registration, deep learning, mask simulation, mask defect categorization, fault detection

## 1. INTRODUCTION

Advancements in deep learning (DL) related to cognitive pattern matching abilities have enabled many recognition and decision tasks in various real-life applications. In particular, in the field of computer vision, state-of-the-art neural networks have been applied to identify and classify objects, synthesize images, improve super-resolution, etc. These deep learning methods have shown promising outcomes. Manufacturing industries are leveraging artificial intelligence (AI), especially deep learning for their smart manufacturing capabilities related to inspection, anomaly detection, machine vision, predictive analysis, and maintenance [13]. Deep learning capabilities have augmented human experts in the field of manufacturing to make better decisions in less time. Mask shops are no different and need to extend similar smart manufacturing capabilities to their SEM-based mask analyses. Since SEM images are pixelated dose maps, almost all the deep learning-based computer vision techniques can be applied to these SEM images for better inspections and analyses. In this paper, we propose three tools for mask analysis by leveraging deep learning techniques.

### 1.1 Three Useful DL Tools

We built three tools for our DL toolset for SEM-based mask analysis. The first is a tool (Fig-1) to automatically filter good quality SEM images using a DL-based binary classifier to filter out good SEM images, particularly for test chips. Because test chips purposefully challenge the limits of the mask process, it is normal to have bad SEM images. The measurement values that are extracted by CD-SEM machines need to reject any such bad images, and those extracted measurements should be ignored in any further analysis.

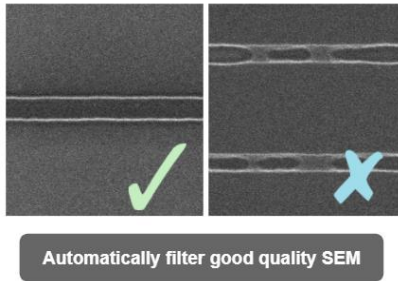


Fig-1: Automatically Identify Good SEM Images and Reject Bad Ones

The second tool (Fig-2) is for aligning CAD and SEM images for applications that require CAD as well as SEM images, where it is important that features on both the images are properly aligned. We built a second DL model to align CAD and SEM images.

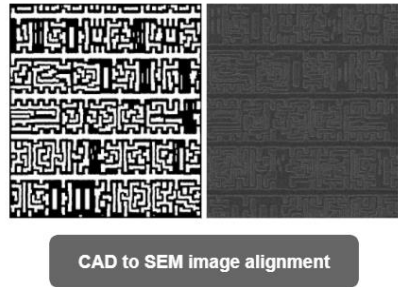


Fig-2: Properly Align Features on CAD with SEM

For the third tool (Fig-3) for VSB-writer defect classification, we used a DL multi-class classifier to categorize various types of VSB mask writer defects.

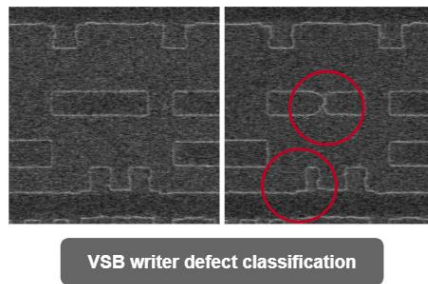


Fig-3: Identify and Classify VSB Mask Writer Defects

All three applications use state-of-the-art deep neural networks. A common challenge for applying deep learning to SEM-based analysis for the mask shops, and for that matter any production-quality deployment of deep learned applications, is that a huge amount of data is required. In the large numbers of images, typically in 100,000s of images, you need good coverage of all types of data including different types of normal data, but also a large number of anomalous data. In general, it's hard to obtain a large number of SEM images. It is even harder to get SEM images with anomalies like defects.

Mask shops are highly skilled and do an incredible job of not creating defective features, so having enough SEM images with a variety of defects to sufficiently train deep learning networks is difficult. A robust alternative is to be able to generate and synthesize the SEM images. For this purpose, we used SEM digital twins described in the next section.

### 1.2 SEM Digital Twins

Deep learning networks are programmed by data, instead of by writing explicit algorithmic code, and hence require large amounts of data [5]. In image-based DL applications, while training the network, one can find a certain set of input images that could confuse the network, and the deep learning engineer fixes the network by finding a new set of images to train the network with better accuracy. DL also needs specific types of SEM images to augment data where the network is confused. So, in the process of improving the performance of deep learning networks, it is critical to be able to collect or generate more types of images where the network is prone to confusion. Because of the difficulty and expense of obtaining enough SEM images from mask shops to do this, the only viable option is to generate SEM images. SEM digital twins can be used to generate any specific type of an SEM image.

A digital twin is a digital clone of a physical entity or a system that is created using mathematical and physics-based modeling. Digital twins offer an efficient way to study and observe the performance and behavior of real-life systems. Based on this concept, as shown in Fig-4 below, we built deep learning-based SEM digital twins to generate realistic-looking SEM images [6]. The SEM digital twins take CAD data, which is a simulated mask pattern, and output corresponding generated SEM data. Different patterns, normal as well as with anomalies having defects, could be induced to CAD data through simulation, and the digital twins can then be used to generate SEM images. The generated SEM images are very similar to real SEM images and can be used for deep learning training.

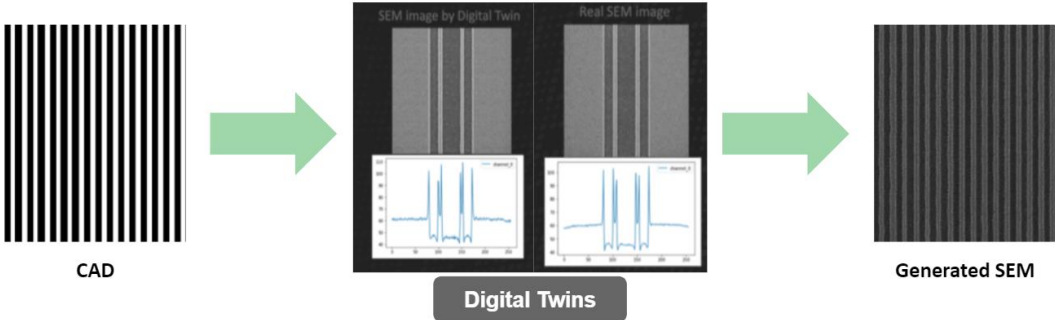


Fig-4: SEM Digital Twins

### 1.3 Millions of SEM Images Generated

Using digital twins, we generated millions of SEM images. These SEM images have regular geometry patterns, as well as patterns with anomalous defects as in Fig-5. Per our knowledge, our digital twins' framework is the first system to generate synthetic SEM images with curvilinear shapes [1].

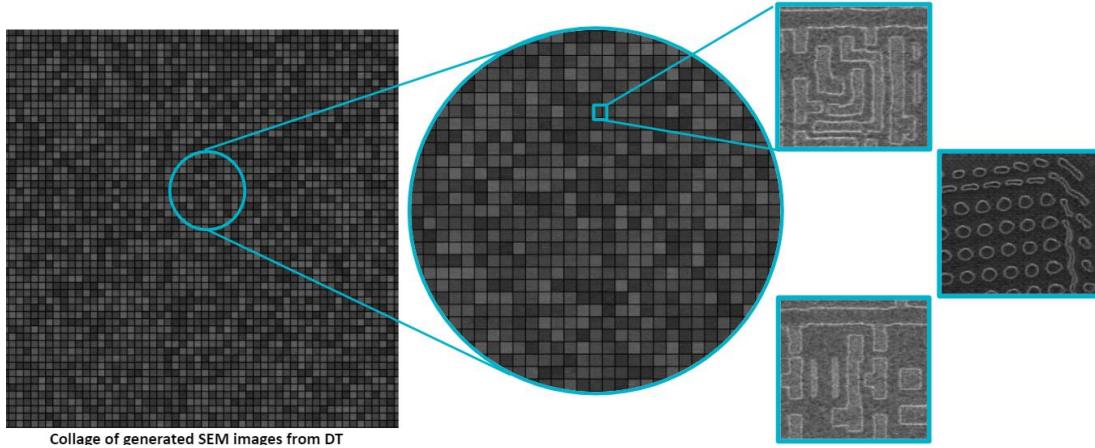


Fig-5: Generated SEM Images with Normal, Defect and Curvilinear Shapes

The next three sections of the paper describe our three DL tools for mask analysis. Each section explains the need for the tool, training and test data used, the underlying DL model, and our results. The second and third tools used and needed SEM digital twins to generate millions of test cases.

## 2. TOOL TO AUTOMATICALLY FILTER HIGH QUALITY SEMS

### 2.1 Need for the Tool

It is normal to have bad SEM images for test chips, because the test patterns purposefully challenge the limits of the mask process. This causes the features to be printed on the mask incorrectly, due to intended and induced problems. For example, a 30nm wide wire will most likely not resolve on the mask when the limit of the process is 40nm. Test chips purposefully contain features smaller than the process limit, because figuring out the process limit requires going over the limit. Engineers also do “through dose” writing to change the dose used in writing the mask by, say, +10%, 0%, -10%. A 30nm wide wire on some processes might print with +10%, but not at all with -10%, and a bad image that can't be measured at 0%. In some cases, features spill over the boundaries of the SEM field of view, resulting into a bad SEM image. Particularly for mask modeling tasks using CD-SEM machines, low fidelity images will need to be ignored in any analysis. Examples of good and bad SEM images are in Figs-6 (a) and (b).

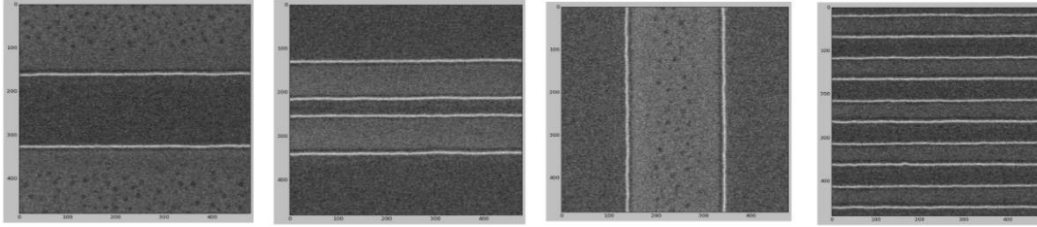


Fig-6 (a): Good SEM Images for a Test Chip

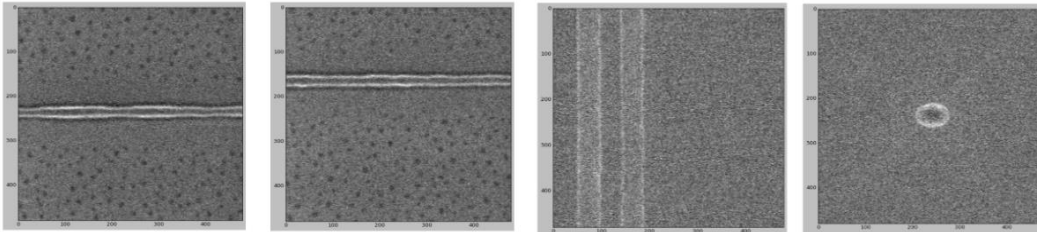


Fig-6 (b): Bad SEM Images for a Test Chip

For reasons described above, it is essential to filter out good quality SEM images before any test-chip analysis. A rule-based method can be applied to filter images. However, because SEM image conditions can change from process to process due to varying noise, contrast, and lighting conditions, rule-based methods are not optimal. Manually filtering SEM images can also be tedious, time consuming and counterproductive. Experts might spend hours filtering good SEM images and still make human errors in classification.

We built a DL-based tool, applying a semi-supervised method to automatically filter good images, which took only minutes to filter 4200 SEM images. By contrast, it took an engineer approximately four and a half hours to filter the same number of images. We started with an accuracy goal in mind of no less than 90%, with a low false negative image filter to ensure that the ratio of good images that are falsely classified as bad (and are unnecessarily discarded) remains low.

## 2.2 Training and Test Data

Because this first DL tool did not require an extremely large amount of data, we did not need to use digital twins. To train the DL model for filtering out good SEM images, the model required only 2723 good SEM images, as shown in Fig-7. For the test, we manually labeled 4226 images (3224 good and 1002 bad images) on which the models' accuracy was tested.

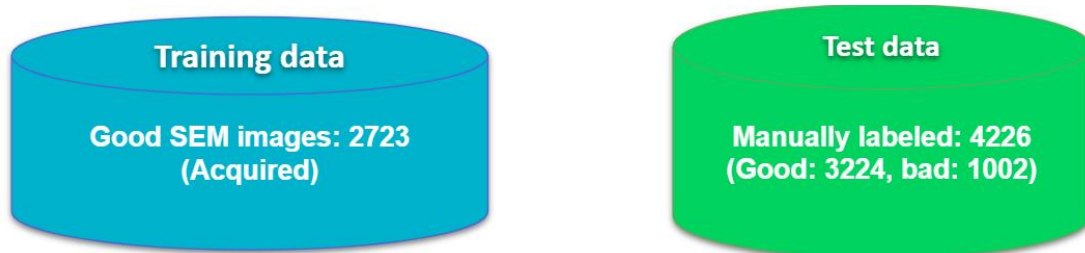


Fig-7: Acquired SEM Images for Training and Test of the Image Filter Tool

### 2.3 Deep Learning Model

A deep autoencoder [7] based DL model followed by an anomaly detection network [8] was used to filter out automatically the good SEM images. To the best of our knowledge, this framework is the first to apply a semi-supervised anomaly detection network along with a deep autoencoder to filter out good quality SEM images. The deep autoencoder was first trained on good SEM images to learn a probability distribution of good SEM image data and produce a vectorized embedding for the images (Fig-8). The trained autoencoder also calculates a reconstruction error which is low for good SEM images and high for bad SEM images. Embedding from the trained autoencoder is combined with the reconstruction error and fed to an anomaly detection network (Fig-9). The output from the anomaly detection network is a probability distribution for good and bad images, which is used to filter the dataset of the images. We call this method semi-supervised since we only used good SEM images to learn the model.

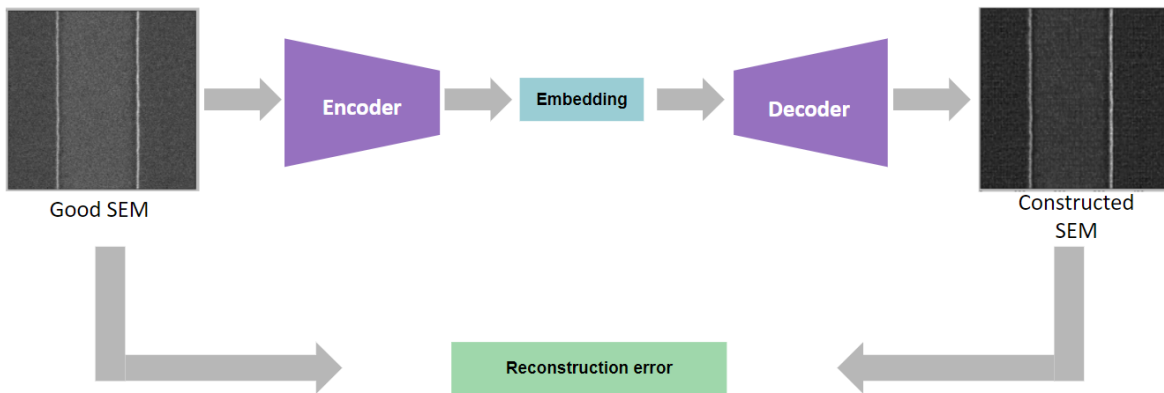


Fig-8: A Deep Autoencoder Trained to Produce Image Embedding and Reconstruction Error

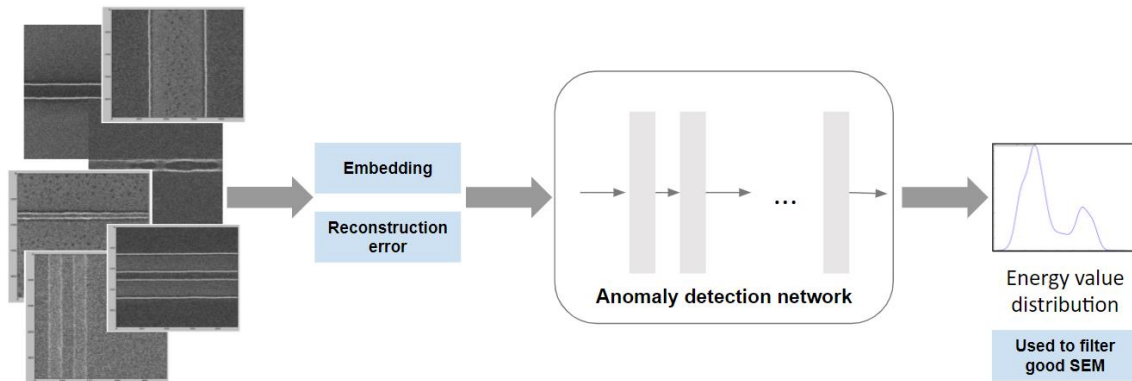


Fig-9: Embedding and Reconstruction Error are Fed to an Anomaly Detection Network

### 2.4 Results

With the filtering tool, we achieved 94.5% accuracy on our test data, with a false negative rate of 5%. Filtering the test images took one minute on a CentOS workstation consisting of a 1080ti GPU. In

comparison, it took hours to manually filter the good SEM images. Fig-10 shows some of the good SEM images filtered by the tool.

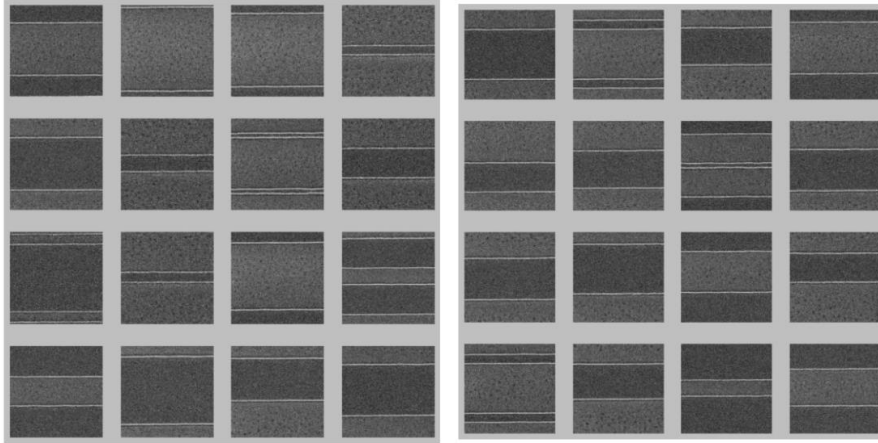


Fig-10: Automatically Filtered Good Images

### 3. TOOL TO ALIGN CAD DESIGNS WITH SEM IMAGES

#### 3.1 Need for the Tool

SEM images taken by the mask shops are often misaligned with the corresponding CAD/design-data in offset, rotation and scaling. For these reasons, for applications such as DL projects that require both CAD data and their resulting SEM images, CAD to SEM image alignment is essential. We encountered this misalignment issue while improving SEM digital twins' accuracy. Improving the digital twins' performance motivated us to build an automatic alignment capability for CAD to SEM images.

While traditional algorithm-based image alignment approaches are available, they are limited, particularly for two different image domains, such as CAD and SEM [9]. For same-domain image alignment, i.e., CAD to CAD or SEM to SEM, existing methods only work for a small range of translation, rotation, and scaling. For cross-domain image alignment, i.e., CAD to SEM, existing iterative and feature extraction-based methods fail to work for most of the translation, rotation, and scaling values. Many DL-based supervised and unsupervised medical imaging methods showed promising image alignment results for the same domain images [17]. A few studies also performed cross-domain image alignment between Magnetic Resonance Imaging (MRI) and Computed Tomography (CT) scan images [10]. They showed promising results with non-rigid image alignment, where local geometries within the image need alignment and learn a non-linear transformation.

We applied a variant of a DL-based image-registration network and quickly saw superior results for CAD to SEM image alignment. Fig-11 shows an example of misaligned CAD and SEM images. In this case, the CAD image needed a transformation to align with the SEM image. Fig-12 shows how our image-alignment trained model aligned the CAD and SEM images.

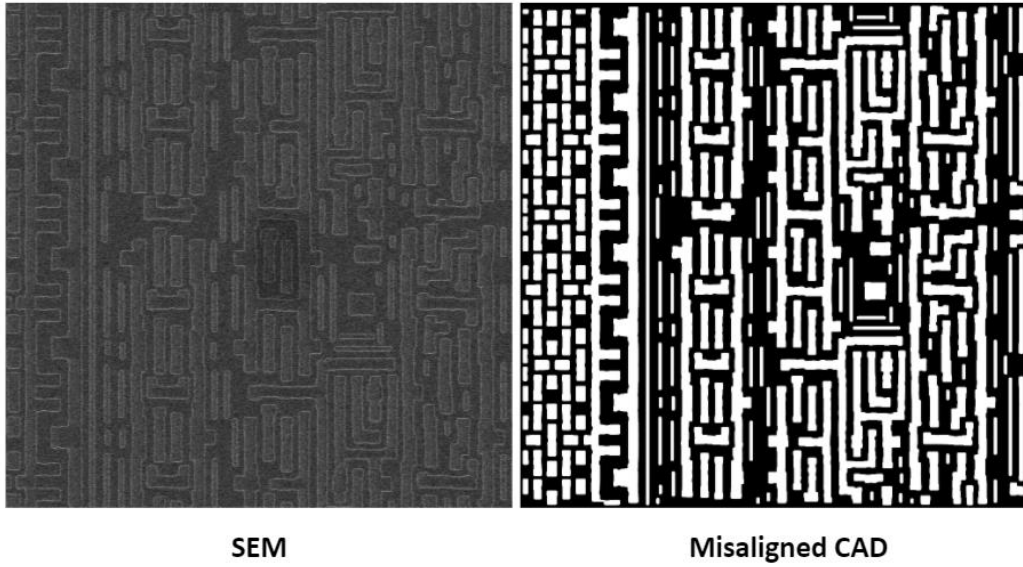


Fig-11: Misaligned CAD to the SEM

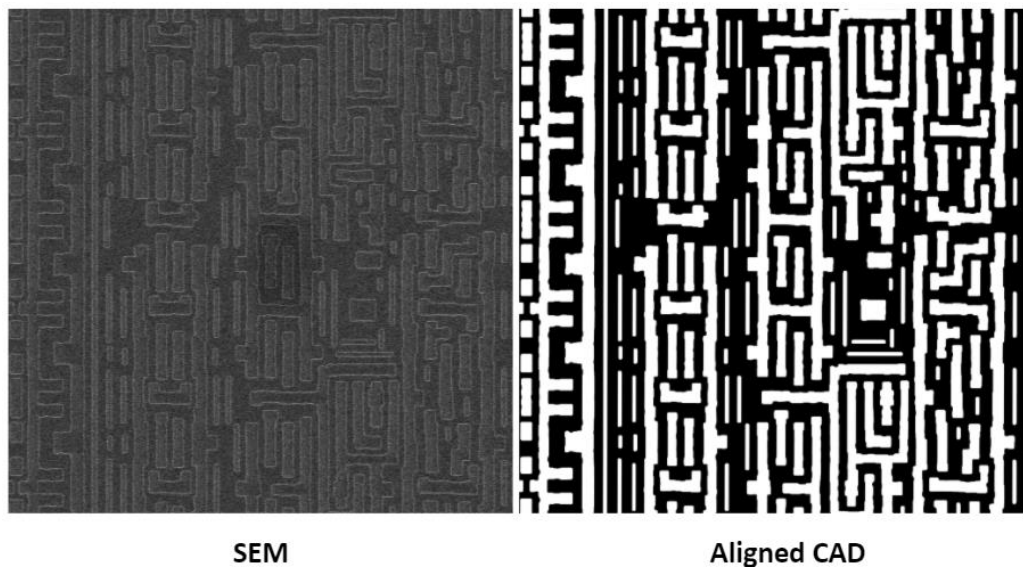


Fig-12: Aligned CAD to the SEM

To visualize how the network performed on alignment, we overlapped CAD and SEM images. Fig-13 on the left shows misaligned images, and on the right aligned images. In misaligned images there are solid filled geometries, where CAD are either partially or not at all overlapped with SEM. Whereas on the right, the solid filled geometries perfectly overlap with SEM.

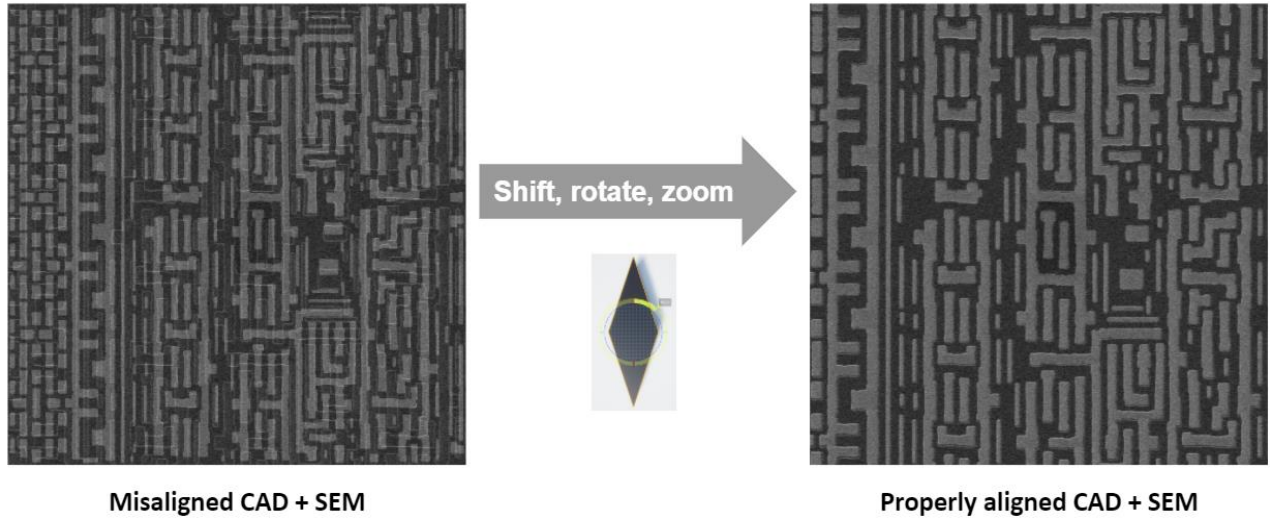


Fig-13: Overlapped CAD and SEM (Left: Misaligned, Right: Aligned)

### 3.2 Training and Test Data

The underlying DL model for CAD to SEM alignment required us to gather at least 700,000 pairs of aligned CAD and SEM images to train the model. Due to physical limitations and resource constraints, obtaining 700,000 SEM images from mask shops was next to impossible. We managed to get these SEM images only through digital twins that generated SEM images. Using the digital twins, we generated a large number of pairs of aligned CAD data and resulting SEM images. We induced misalignment by applying transformations such as scaling, rotation, and translation with a varying range of values for transformation. Finally, using a combination of digital twins and OpenCV [11], we generated enough training data (Fig-14) to train our image alignment model.

To test the model (Fig-14), we generated 70,000 test images from the digital twins. We also manually aligned 185 real SEM images to see how the model performed on real SEM images.

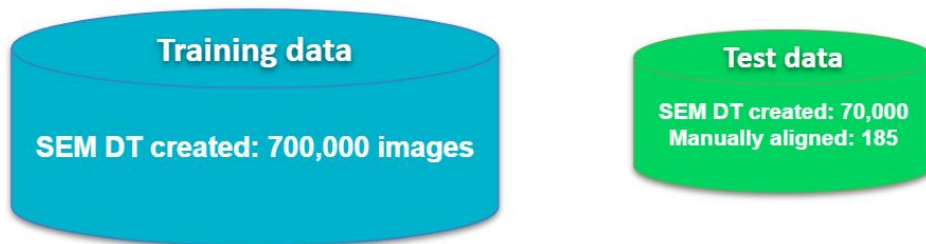


Fig-14: Training and Test Data for CAD to SEM Image Alignment

### 3.3 Deep Learning Model

Inspired by image registration in other fields [10], we developed a custom deep neural network to align CAD to SEM images for this tool. As shown in Fig-15, the registration network comprises a convolution neural network (CNN) for feature extraction from misaligned and aligned CAD and SEM images, followed by a feed-forward network to learn spatial transformation such as translation, rotation, and zoom-in, zoom-out values. The network used a custom loss function to optimize the model, which takes the difference between aligned cad and the output after applying spatial transformation on misaligned cad.

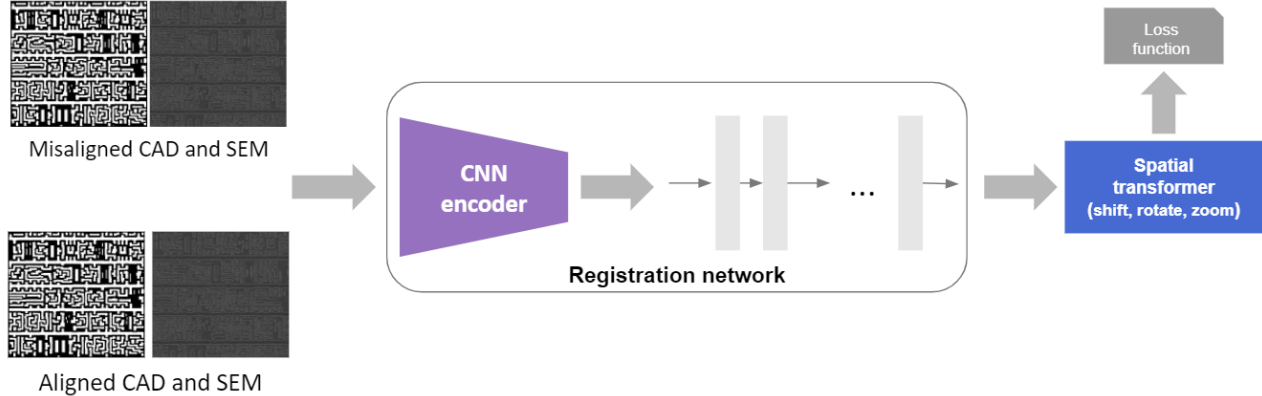


Fig-15: Architecture of the CAD to SEM Image Alignment Network

### 3.4 Results

We visually inspected overlapping CAD and SEM images and could see extremely good alignment done by the DL model. Quantitatively, we used a 1-NCC (Normalized Cross Correlation) score [12]. NCC captures pixel-wise similarity between two images. In our case, a score of 1 means the two images are perfectly aligned and a score of 0 means they are completely misaligned. On our manually aligned test images, we saw an average 0.9 NCC score. Examples of alignments of CAD and SEM images are shown in Figures-16 (a-e), where the DL-model shows promising results.

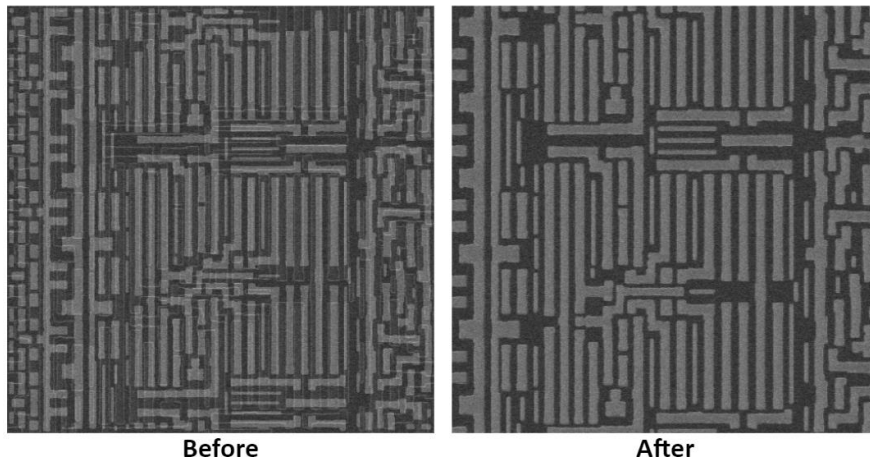


Fig-16 (a): Case-1: NCC Score of 0.9934

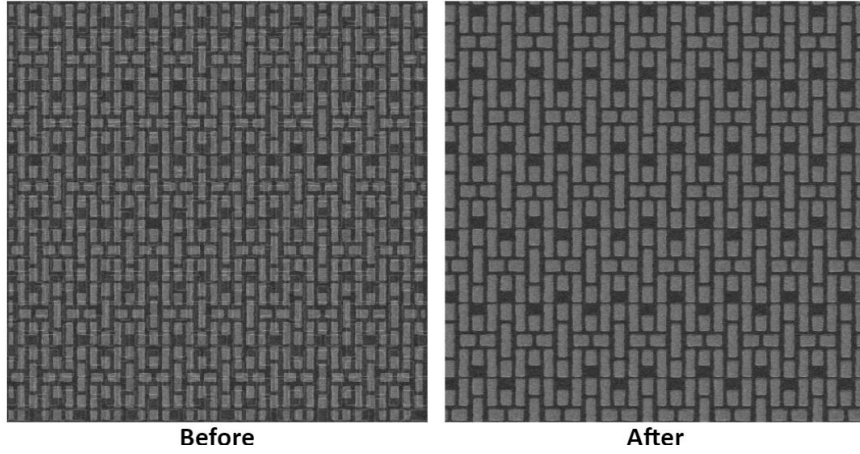


Fig-16 (b): Case-2: NCC Score of 0.9905

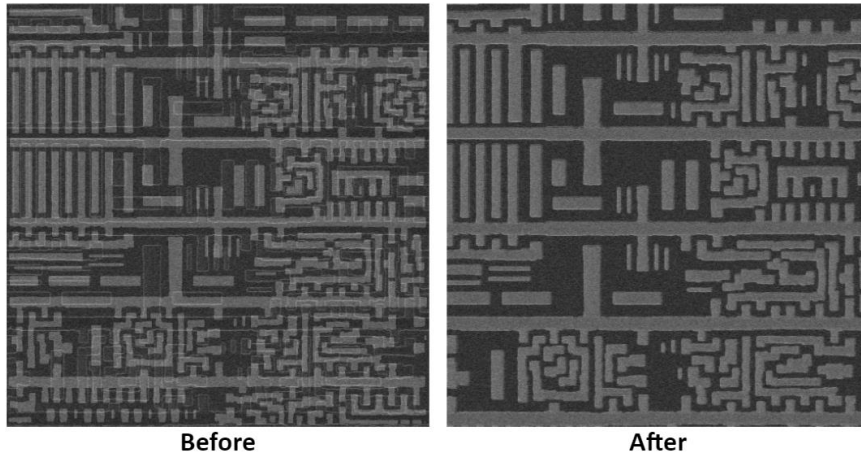


Fig-16 (c): Case-3: NCC Score of 0.9891

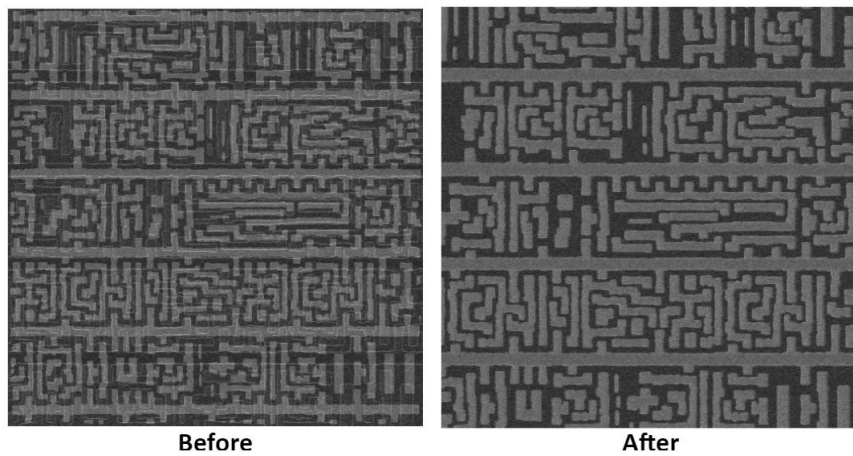


Fig-16 (d): Case-4: NCC Score of 0.9881

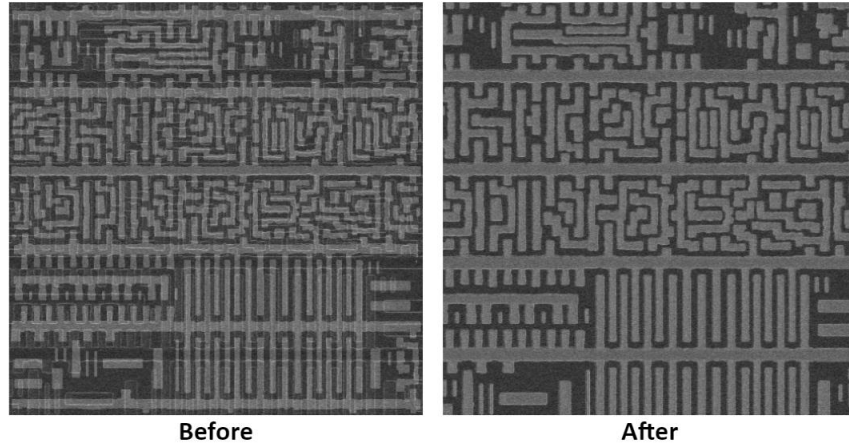


Fig-16 (e): Case-5: NCC Score of 0.9846

#### 4. DEFECT CLASSIFIER FOR VSB WRITERS

##### 4.1 Need for the Tool

Variable Shaped Beam (VSB) mask writer systems are incredibly reliable machines that write mask patterns 24 hours a day, 7 days a week. On rare occasions these systems show wear and tear, such as aging parts, which might cause errors in printing. It is important to quickly diagnose these errors, debug and fix them, and put the machine back to operation as soon as possible. When an error occurs, expert field application engineers must collect relevant information such as log files, history of the equipment, and SEM images containing defect patterns for the diagnosis. The SEM images are one of the most crucial pieces of information that engineers use to identify and classify the defect and further diagnose which component in the VSB writer machine caused the error to occur. This process is tedious and time-consuming. We built a third tool to classify such defects in VSB writers. This DL tool uses SEM images to identify errors in the same manner that engineers use to debug the errors and fix them. Fig-17 shows the architecture of a typical VSB writer.

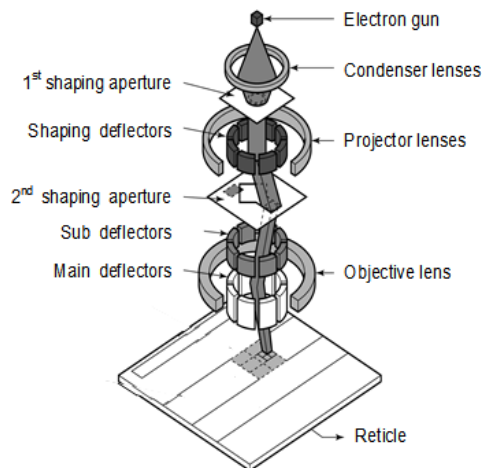


Fig-17: Architecture of a Typical VSB Mask Writer (Courtesy NuFlare)

Electrons are fired in shots, patterning the mask in rectangular or triangular shapes through the VSB writer. A column of a VSB writer principally has three components. First, an electron gun forms an electron beam. Second, the upper part consists of the first shaping aperture, shaping deflectors, and the second shaping aperture. Shaping deflectors are responsible for moving the beam onto the second shaping aperture to create different VSB shapes, either rectangular or triangular. The upper part is also responsible for controlling the shots' size. The third component or lower part consists of two or more deflectors, ensuring accurate shape positioning on the mask.

Problems in any of these components of the VSB writer can cause errors while printing. For example, due to an issue in the electron gun, dose intensity can vary, causing a lower dose margin and the geometries to shrink (Fig-18 (a)). A problem with the sub deflectors in the lower part of the machine could cause shots to be printed at wrong positions, resulting in a position error (Figure 18 (b)). Similarly, a problem in the shaping deflectors in the upper part of the machine can cause distorted shapes on the mask, resulting in a shaping error (Fig-18 (c)).

Our VSB defect classifier tool takes a defective SEM image as input and classifies it as a dose error, shape error, or position error. We also used the first two tools in the toolset along with this third tool to filter good images from the set of real SEM images, and to align CAD and SEM images to improve the accuracy of the SEM digital twins.

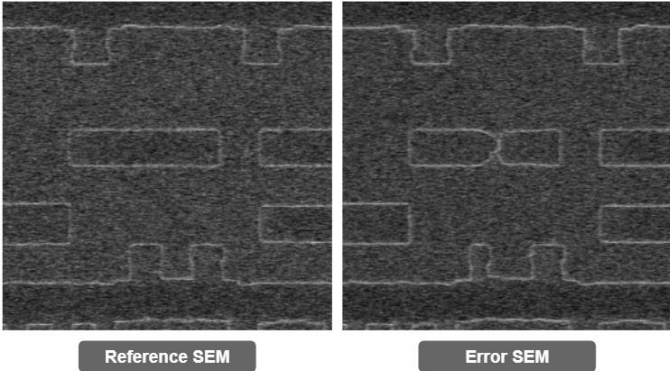


Fig-18 (a): Dose Error

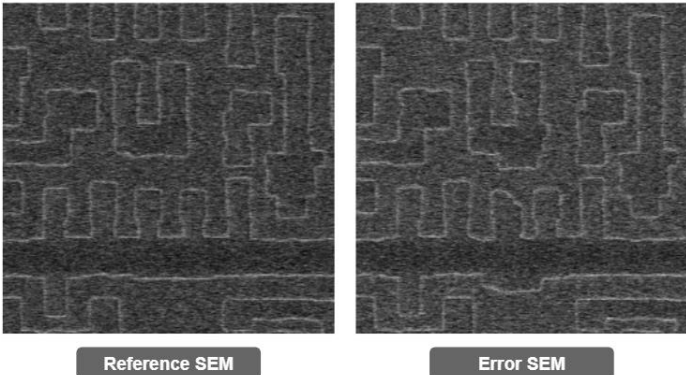


Fig-18 (b): Position Error

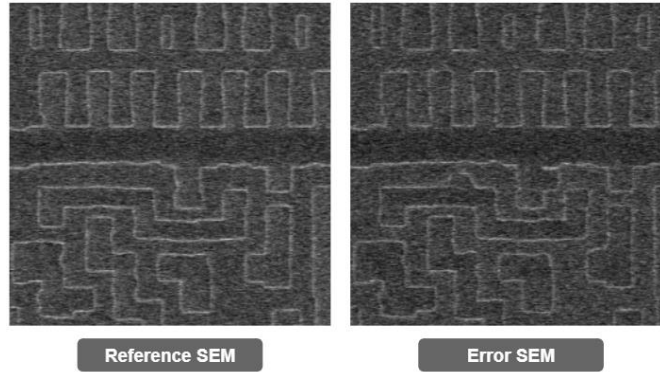


Fig-18 (c): Shape Error

## 4.2 Training and Test Data

Creating the training data for the VSB defect classifier’s DL model turned out to be one of our most intriguing challenges. It’s impractical to get SEM images with all three types of dose, shape, and position errors, let alone specific subtypes of each error category. For example, a dose error could occur in various patterns and for a large number of varying dose intensities. Likewise, a position error occurs due to a permutation and combination of shifting shots from their original position. Similarly, a shape error could occur due to the removal or resizing of shots in varying conditions. It was essential to induce and simulate all possible states and conditions for each error type. Furthermore, different resist types, etching variations in printing, and other variations in images captured by SEM machines make this problem challenging to model using deep learning.

We used TrueMask® DS, a GPU-accelerated mask-wafer double simulation platform offered by D2S, to simulate various error types, followed by the SEM digital twins to generate more than one million SEM images covering regular patterns and all three types of defects (Fig-19). Our observation is that DL can learn features from the SEM images generated using digital twins, then use that learning to find defects on real SEM images. Rarely, we observed that digital twins could not embed some peculiar noise and line edge roughness to output SEM images similar to the actual SEM images. In these cases, we needed to ingest a minimal number of real SEM images, so that the DL classification model could “see” these rare SEM images for learning. For the test, we printed masks with induced errors and took more than 2000 real SEM images. Expert application engineers at NuFlare manually annotated 250 real SEM images by crowdsourcing used for model evaluation (Fig-19).



Fig-19: More than 1M images were generated using DT. More than 2K SEM images were taken from printed masks.

### 4.3 Deep Learning Model

A typical DL-based image classifier inspired the DL model for the VSB defect classification task. We tried VGGNet [14] and ResNet [15] neural networks first, which didn't work out of the box. We then used a custom variant of ResNet architecture that consists of multiple convolutional layers with skip connections across them for feature extraction, and a few fully connected layers for spitting out the error category probabilities. Reference and defect SEM images are input to the DL model, which outputs a probability that the error belongs to one of the three error classes or is normal.

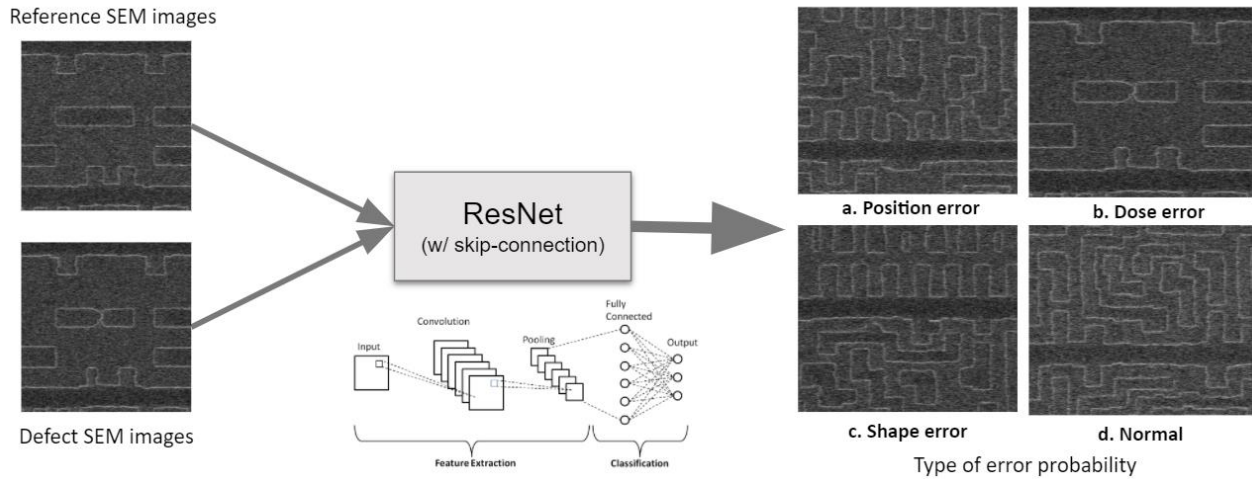


Fig-20: Architecture of VSB mask defect classifier

### 4.4 Results

The DL model for the defect classifier for VSB writers showed promising results on the test data. When we compared the DL model's results with human labels, we found that they were equivalent. We also found evidence that human labels were biased towards the types of errors the application engineers had seen in the past. The DL model results were more neutral. This was only possible because we were able to complete the DL training with more than a million SEM images with a large variety of the errors in each category using digital twins.

Figs-21 (a) and (b) show two types of examples from our results: a position error and a shape error. There are four images for each example: from left to right, the reference SEM image, the error SEM image, a heat map visualization that shows what the neural network sees in the input SEM image, and finally the probabilities of each error occurring as estimated by the model. As these examples show, the network is able to focus on the region where the error persists in the SEM, and there is a 95% or greater probability the model assigned the correct error category. We found the network visualization extremely useful.

Fig-21 (c) shows an example where the DL model gives almost equal probability of 45% and 55% respectively that a dose or shape error exists. This example reflects a complex situation where it is hard for the network to discern and differentiate between the error categories. When checked with the expert engineer, it turned out that these kinds of errors were hard even for them to classify.

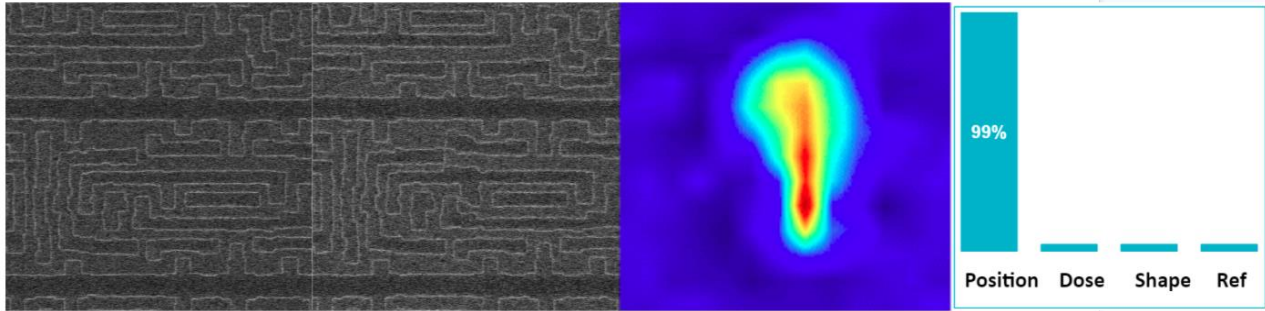


Fig-21 (a): Example of Position Error

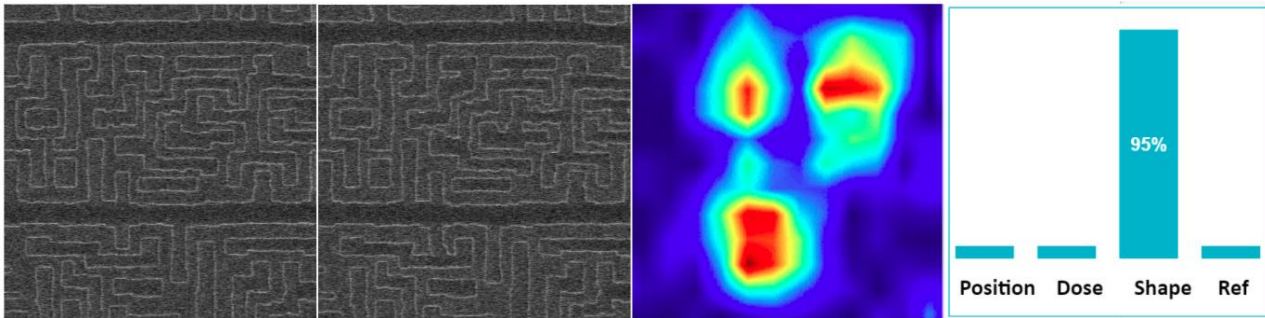


Fig-21 (b): Example of Shape Error

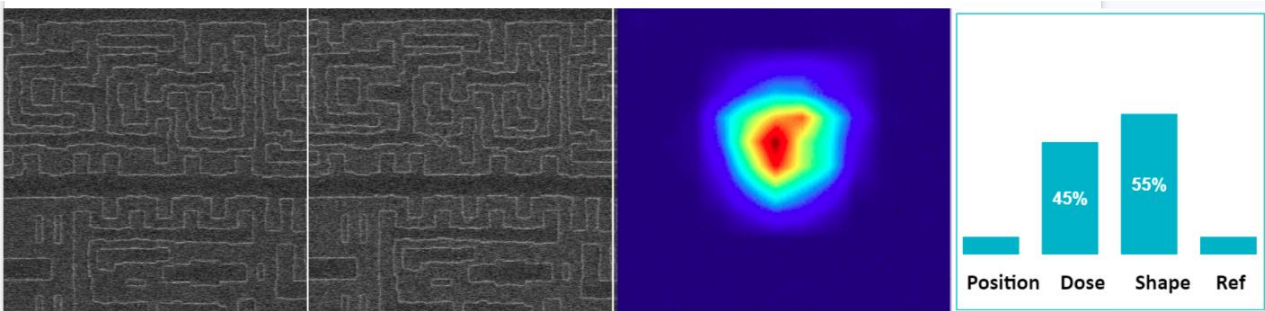


Fig-21 (c): Example of Dose and Shape Errors Being Equally Identified

#### 4.5 VSB Writer Defect Classifier Dashboard

What is a DL tool without being used in production? We built a dashboard to deploy the DL model for the defect classifier in production. While the work is still ongoing, some of the application engineers already find this extremely useful. A view of the tool's dashboard is shown in Fig-22. The dashboard's features include giving users the opportunity to upload a dataset of defect SEM images, to select a specific DL model to run the inference on it, and to visualize the prediction performance of the tool right there.

This dashboard is built using Plotly [16], a data-science application tool for creating web-based dashboards. The dashboard can be hosted on on-premise workstations for internal use by customers or vendors.

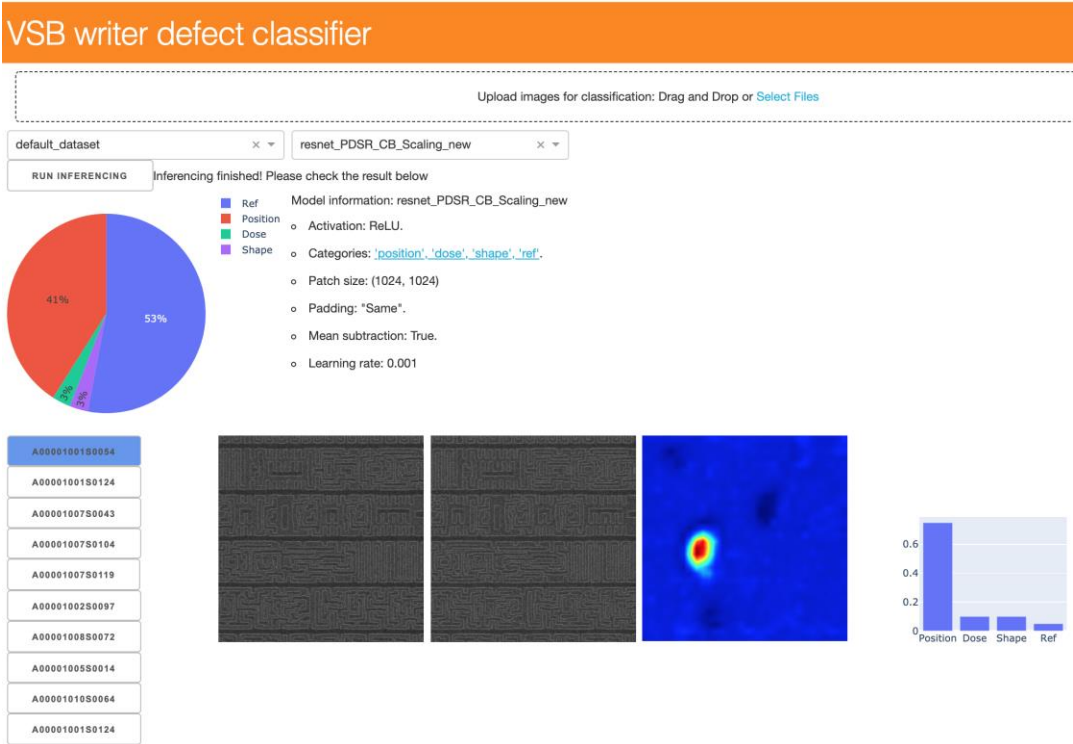


Fig-22: VSB Writer Defect Classifier Dashboard

#### 4.6 Generalization to Classifying Other SEM-based Defects

We used the same digital twins that were used for VSB mask writer defect classification to generate approximately 36,000 synthetic SEM images reflecting various defects found in real SEM images, then used them as training data for another classification model. Fig-23 shows some generated SEM images from the SEM digital twins, including one that has a feature resize defect. For the test, first we validated the model using images generated from digital twins, then we showed the ability of the model to generalize over the real SEM images with errors as shown in Fig-24.

In the case shown in Fig-24, we wanted to classify feature resize errors in real SEM images. We again used the SEM digital twins to generate synthetic SEM images, trained a classification model on them, and applied the trained model to real SEM images. These tasks show the strength of using digital twins to generate various kinds of data with defects and using the synthesized generated data to train a DL model.

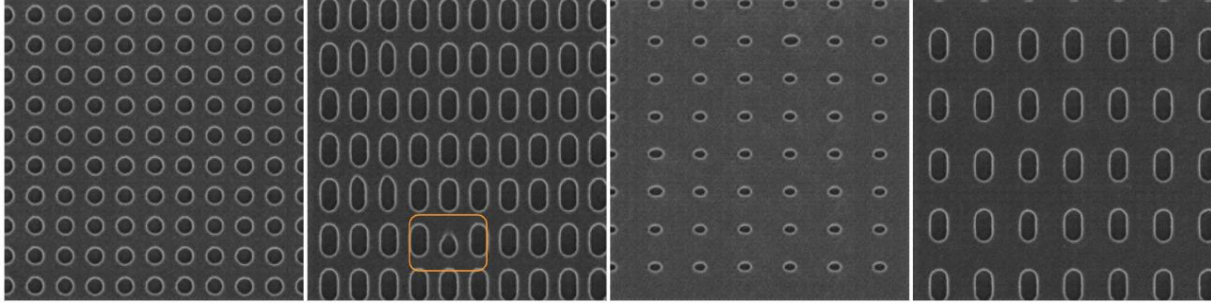


Fig-23: Generated SEM Images. Second image has a feature resize defect.

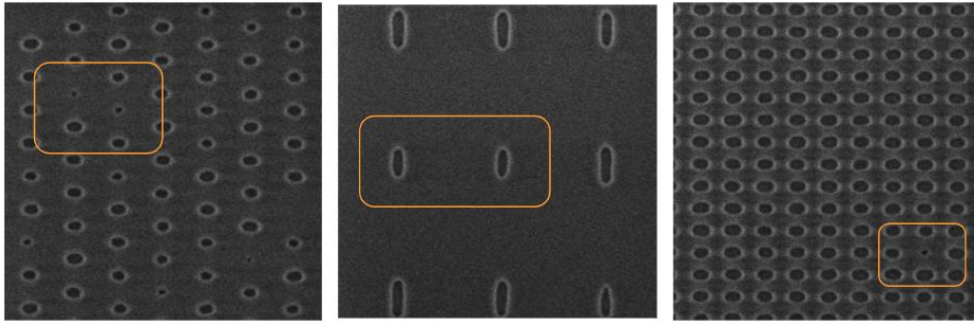


Fig-24: Real SEM Images with Feature Resize Errors

Fig-25 shows the DL model used for classifying real SEM images with feature resize errors. For this task, we used a custom ResNet [15] architecture.

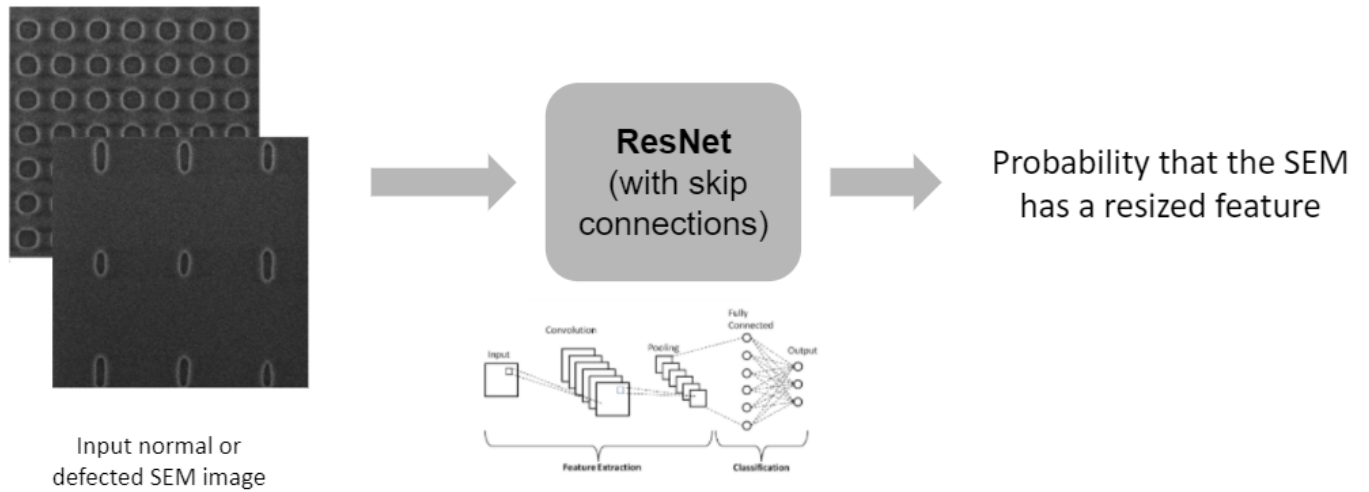


Fig-25: ResNet based classification network

With the trained classifier, we saw promising results with reasonable network performance with classification accuracy of 94% on the digital twins' generated test data and accuracy of 90% on the real SEM test images. In addition, we had high confidence in the network visualization on real SEM error images as shown in Fig-26.

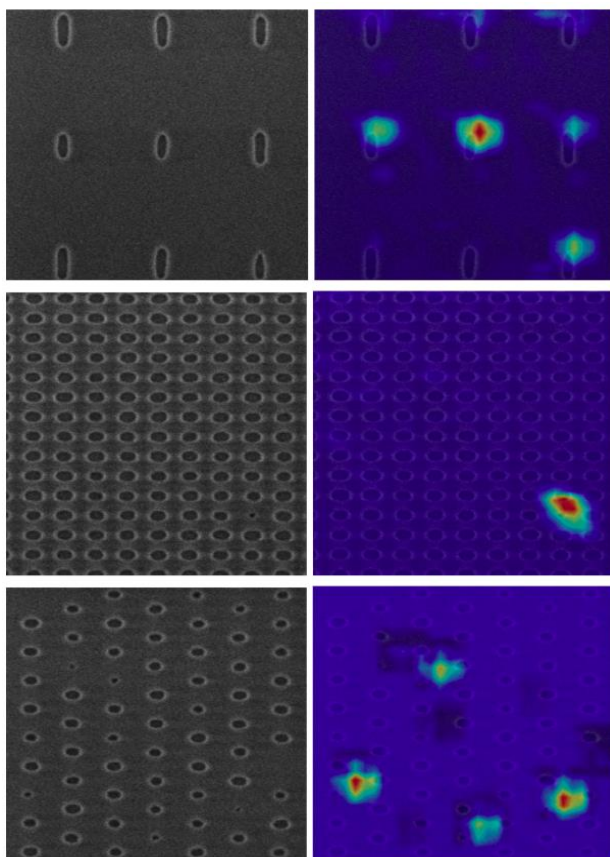


Fig-26: Network Visualization on Real SEM Error Images

## 5. CONCLUSION

The promising results from the three DL tools in the (Fig-27) toolset demonstrate the power of deep learning for mask analysis using SEM images. The fact that we used the first two tools to increase the performance of the third one emphasizes that DL-based tools are a great asset in the mask analysis arsenal. You can build tools one by one, or apply them on top of others.

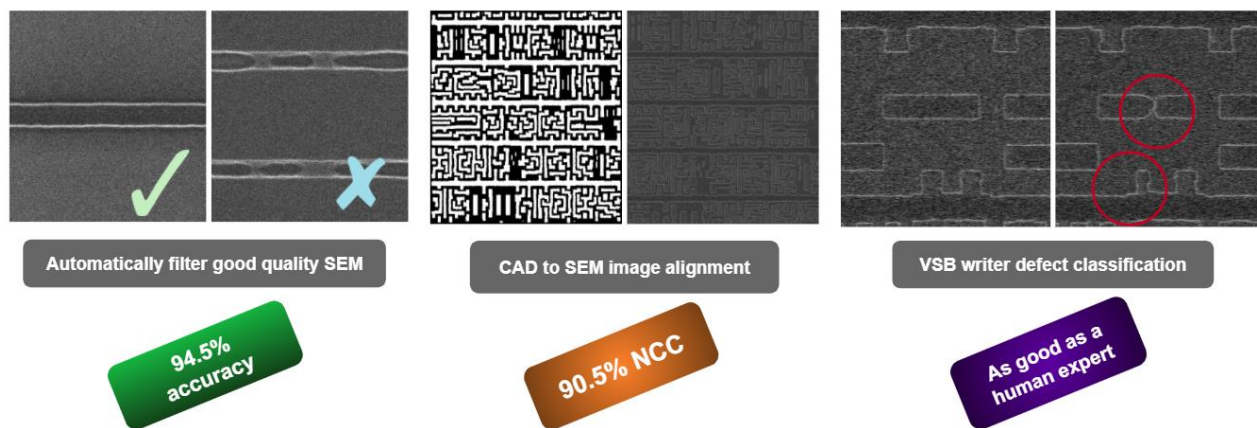


Fig-27: Promising Results with the Three Tools

Further, digital twins are essential when it comes to harnessing DL to improve the manufacturing process. Without an ability to generate millions of images, particularly images of anomalous data, DL engineers must go back to the mask shop or the fab to print more cases and take more SEM images which is not practical and impedes production.

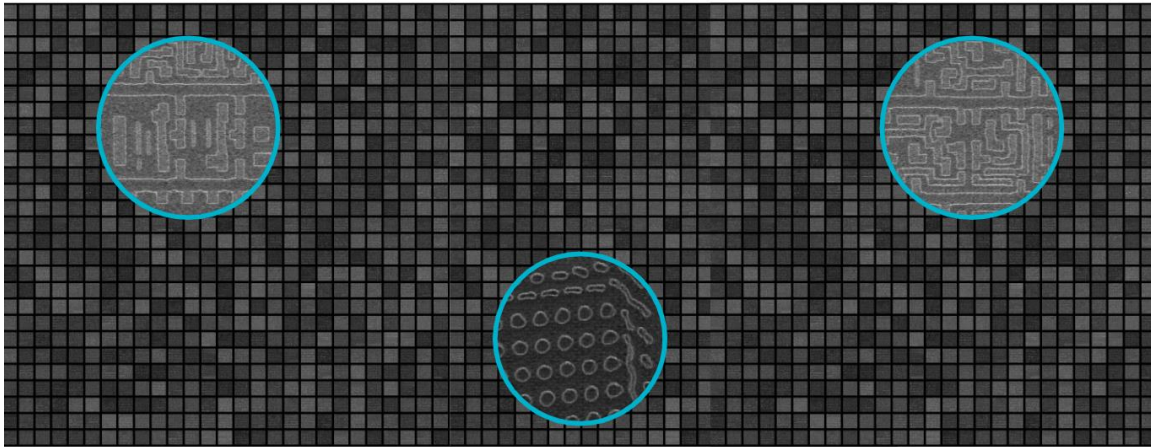


Fig-28: Collage of Millions of SEM Images Highlighting Patterns with Curvilinear Shapes

In these cases, deep learning was able to effectively alleviate some of the tedious and error prone processes that humans perform today. But DL can only succeed if digital twins are there to generate ALL of the specific training data you need.

## REFERENCES

- [1] Pang, Linyong, et al. "Making digital twins using the Deep Learning Kit (DLK)." Photomask Technology 2019. Vol. 11148. International Society for Optics and Photonics, 2019.
- [2] Chaudhary, Narendra, Serap A. Savari, and S. S. Yeddulapalli. "Automated rough line-edge estimation from SEM images using deep convolutional neural networks." Photomask Technology 2018. Vol. 10810. International Society for Optics and Photonics, 2018.
- [3] Chaudhary, Narendra, Serap A. Savari, and Sai S. Yeddulapalli. "Line roughness estimation and Poisson denoising in scanning electron microscope images using deep learning." Journal of Micro/Nanolithography, MEMS, and MOEMS 18.2 (2019): 024001.
- [4] Midoh, Yoshihiro, and Koji Nakamae. "Image quality enhancement of a CD-SEM image using conditional generative adversarial networks." Metrology, Inspection, and Process Control for Microlithography XXXIII. Vol. 10959. International Society for Optics and Photonics, 2019.
- [5] Baranwal, Ajay, et al. "Deep learning primer: data is the new source code (Invited Paper)", Proc. SPIE 108101, Photomask Technology 2018.
- [6] Baranwal, Ajay, et al, "Five deep learning recipes for the mask-making industry." Photomask Technology 2019. Vol. 11148. International Society for Optics and Photonics, 2019.
- [7] Hinton, Geoffrey E., and Ruslan R. Salakhutdinov. "Reducing the dimensionality of data with neural networks." science 313.5786 (2006): 504-507.
- [8] Zong, Bo, et al. "Deep autoencoding gaussian mixture model for unsupervised anomaly detection." International Conference on Learning Representations. 2018.
- [9] Meng, Qingjie, Daniel Rueckert, and Bernhard Kainz. "Unsupervised Cross-domain Image Classification by Distance Metric Guided Feature Alignment." arXiv preprint arXiv:2008.08433 (2020).
- [10] Cao, Xiaohuan, et al. "Deep learning based inter-modality image registration supervised by intra-modality similarity." International Workshop on Machine Learning in Medical Imaging. Springer, Cham, 2018.

- [11] Culjak, Ivan, et al. "A brief introduction to OpenCV." 2012 proceedings of the 35th international convention MIPRO. IEEE, 2012.
- [12] Zhao, Feng, Qingming Huang, and Wen Gao. "Image matching by normalized cross-correlation." 2006 IEEE International Conference on Acoustics Speech and Signal Processing Proceedings. Vol. 2. IEEE, 2006.
- [13] Yao, Xifan, et al. "From intelligent manufacturing to smart manufacturing for industry 4.0 driven by next generation artificial intelligence and further on." 2017 5th international conference on enterprise systems (ES). IEEE, 2017.
- [14] Simonyan, Karen, and Andrew Zisserman. "Very deep convolutional networks for large-scale image recognition." arXiv preprint arXiv:1409.1556 (2014).
- [15] He, Kaiming, et al. "Deep residual learning for image recognition." Proceedings of the IEEE conference on computer vision and pattern recognition. 2016.
- [16] Plotly Technologies Inc. Title: Collaborative data science Publisher: Plotly Technologies Inc. Place of publication: Montréal, QC Date of publication: 2015 URL: <https://plot.ly>
- [17] Balakrishnan, Guha, et al. "An unsupervised learning model for deformable medical image registration." Proceedings of the IEEE conference on computer vision and pattern recognition. 2018.